BMC Methods

METHODOLOGY

Open Access

An optimised protocol for the relative quantification of ATP and polyphosphates in the microalga *Chlamydomonas reinhardtii* and other microorganisms

Eliora Israelievitch[1] and Alix Boulouis[1*]

Abstract

Background Polyphosphates (polyP) and ATP are phosphate-containing metabolites present in prokaryotes and eukaryotes. PolyP are synthesised from ATP and have a wide variety of functions including phosphate and cation storage. In most microorganisms, a role of polyP in energetic metabolism has not been investigated. In the green microalga *Chlamydomonas reinhardtii*, polyP synthesis was suggested to buffer ATP concentration. To uncover polyP participation in energetic metabolism, relative quantification of both metabolites is needed. ATP and polyP half-lives differing greatly, harvesting generates biases in the relative quantification of these metabolites in current methods. We present here a protocol optimised to obtain maximal yield and integrate assay constraints linked to metabolite stability and purity.

Methods Our optimised method quantifies ATP and polyP from the same cell extract, obtained by neutral phenol–chloroform extraction of cells directly pipetted from their culture. After a second chloroform extraction, ATP is quantified directly from the extract, while polyP measurement requires purification by ethanol precipitation. We tested statistical effects in our results with t-test, one-way analysis of variance or Kruskall-Wallis testing and appropriate post hoc testing.

Results We show that the polyP/ATP ratio of the reference *C. reinhardtii* strain CC-4533 in exponential mixotrophic growth is around 70. The optimised protocol performs as well as specific protocols for either ATP or polyP measurements. Direct sampling from the culture works better than centrifugation to maintain physiological conditions and ATP content. Using spiking, we show that ATP is fully recovered. PolyP with 3 P units are poorly recovered (25%) while chains of 14 units and above are fully recovered. The method also works for other microorganisms, including yeast, diatoms and cyanobacteria. Finally, we show that the polyP chain length distribution extracted from CC-4533 is broad, reaching up to several thousand P with a mean around 200 P.

Discussion Our protocol using neutral phenol–chloroform extraction on directly harvested samples allows quantification of true physiological ATP and polyP cell concentrations, and calculation of the polyP/ATP ratio from low-density samples with no other normalisation. It can be applied to other microorganisms or cells to investigate polyP physiology in a variety of physiological and stress conditions.

*Correspondence:
Alix Boulouis
alix.boulouis@sorbonne-universite.fr

© The Author(s) 2025. **Open Access** This article is licensed under a Creative Commons Attribution 4.0 International License, which permits use, sharing, adaptation, distribution and reproduction in any medium or format, as long as you give appropriate credit to the original author(s) and the source, provide a link to the Creative Commons licence, and indicate if changes were made. The images or other third party material in this article are included in the article's Creative Commons licence, unless indicated otherwise in a credit line to the material. If material is not included in the article's Creative Commons licence and your intended use is not permitted by statutory regulation or exceeds the permitted use, you will need to obtain permission directly from the copyright holder. To view a copy of this licence, visit http://creativecommons.org/licenses/by/4.0/.

Keywords Polyphosphate, ATP, *Chlamydomonas reinhardtii*, Physiology, Bioenergetics, Phenol–chloroform extraction, Harvesting

Introduction

Polyphosphates (polyP) are polymers of inorganic phosphate (P) believed to have pre-existed life on Earth [1]. From phosphate and cation storage to cell signalling and stress response, polyP have a wide range of functions in cells [2, 3]. PolyP are found in all life kingdoms, but their synthesis differs between prokaryotes and eukaryotes [3]. In eukaryotes, the vacuolar transporter chaperone enzyme (VTC) polymerises polyP from ATP [3]. ATP also has a central role in cellular bioenergetics, and provides energy in numerous metabolic reactions, making ATP concentration critical to cell physiology. In the green microalga *Chlamydomonas reinhardtii*, a model species for bioenergetics, a mutant without the VTC enzyme accumulates higher levels of ATP, in conditions where the wild-type produces polyP [4]. This led Sanz-Luque et al. to suggest that polyP synthesis allows to buffer the excess ATP in *C. reinhardtii* [4]. This way, synthesizing polyP allows to decrease the ATP/ADP ratio during nutrient starvation, which is required to maintain functional electron transfer chains in the chloroplast and mitochondria, allowing proper acclimation to take place [4]. Additionally, a participation of polyP in energy storage in eukaryotic cells has been suggested [4, 5]. This participation would have to be indirect, for example via a phosphate gradient through the acidocalcisome membrane, since the mechanism of the VTC enzyme does not appear to be reversible to regenerate ATP from polyP and ADP [6]. To test the hypothesis that polyP regulate cell bioenergetics, quantifying the relative amounts of polyP and ATP with high accuracy in cells is required. In order to achieve this, the extraction method should be as similar for both metabolites as possible, in order to avoid biases introduced by the different steps of cell harvesting, extraction itself and purification. Stability of both metabolites should be taken into account at each step of the protocol, as well as assay-related constraints.

C. reinhardtii is a model organism of choice to work on the metabolism of polyP. Bioenergetics, including photosynthesis, respiration and primary carbon metabolism, are well studied in *C. reinhardtii* [7–9]. Additionally, versatile genetic tools including all three genome transformations [10], CRISPR targeted modification of the nuclear genome [11] and a MoClo system [12] are available in *C. reinhardtii*. Finally, microalgae of the *Chlamydomonas/Cryptomonas* genus have been found to accumulate polyP in wastewaters [13] and the metabolism of polyP in their model relative *C. reinhardtii* has recently been the focus of the work of several groups [4, 14, 15]. Other photosynthetic micoorganisms store polyP and are more pertinent to study the biogeochemical phosphorus cycle, such as cyanobacteria and diatoms [16–18].

Several protocols already exist to extract and quantify either ATP or polyP, mainly consisting in their separation from the protein fraction. For ATP, the extraction is usually based on acids like trichloroacetic acid (TCA) or perchloric acid [19, 20]. However, Chida et al. showed on mammalian tissues and blood cells that a neutral phenol–chloroform based extraction is more efficient [21]. For polyP, early extraction protocols (in the 1980's and 1990's) have been based on acids (mainly trichloroacetic acid, TCA), carbon tetrachloride or phenol–chloroform, although only the latter properly retrieved granular polyP [22, 23]. More recently, two groups optimised a polyP extraction method in *Saccharomyces cerevisiae* based on neutral phenol–chloroform, decreasing the number of steps from five to one, while increasing the efficiency by 40% [24, 25]. Thus, a neutral phenol–chloroform-based extraction method seems suitable for both ATP and polyP. In this method, variability comes from the imprecise retrieving of the aqueous phase at each extraction step. This becomes irrelevant for the relative quantification of ATP and polyP, alleviating the need of a common normalisation. Indeed, normalisation usually uses cell count, chlorophyll concentration or dry mass, all parameters that can vary with cell cycle, light and nutrient conditions [26].

Biological material harvesting is a key step of metabolite extraction. This is especially true for microorganisms growing in liquid cultures, since the metabolite concentrations of the whole culture are largely diluted by the medium. ATP, a very short-lived metabolite in physiological conditions [27], requires a quasi-instantaneous harvesting and quenching method. Direct sampling of *C. reinhardtii* cells from their culture medium has been previously used, rapidly mixing the algal culture with cold methanol [28]. Indeed, direct sampling allows to avoid steps of culture harvesting, centrifuging and resuspension of cells in the usual harvesting by centrifugation, that would introduce massive changes in physiological conditions of the cells, as well as variability in carrying out these steps. On the contrary to ATP, polyP are more stable metabolites that can be extracted after steps of cell centrifugation and washing [25]. This procedure ensures that only intracellular

polyP are taken into account in the measurement and that Pi contained in the medium does not contaminate the Pi-based spectrophotometric assay of polyP after hydrolysis to Pi. Another option to eliminate medium and cell Pi contribution to the assay is to purify polyP from the cell culture extract by ethanol precipitation [24]. In order to use this method, one should check that this additional step specific to polyP does not introduce a bias in the relative quantification of ATP and polyP. Moreover, centrifugation and washing might or not affect *C. reinhardtii* polyP stocks, but will surely have an impact on cell physiology by changing light intensity, oxygen availability and medium composition, thus representing a potential threat to correct ATP quantification. Therefore, we also tested the influence of the cell harvesting method on our extraction protocol.

We optimised a method to measure physiological concentrations of ATP and polyP in CC-4533 *C. reinhardtii* cells, largely inspired by Chida et al. [21] for the extraction part, and we compared it with other available protocols. We demonstrate the efficiency of the optimised method for both metabolites. We studied the impact of the cell harvesting method on the final ATP and polyP quantifications and on cell physiology. We show that using a precipitation step after extraction allows to purify polyP from contaminating Pi without affecting total polyP quantification, thus allowing to directly harvest cells in their culture medium. Additional minor optimisation steps concerning EDTA concentration and sample storage are also described. The resulting joint extraction protocol for ATP and polyP thus offers the possibility to calculate polyP/ATP ratios independently of any normalisation method. We applied this method on other microorganisms and compared our results with ATP and polyP contents reported in the literature.

Methods

Chemicals

All chemicals used were of analytical grade and all dilutions were made with high purity deionized water (18 MΩ cm resistivity) obtained from a milliQ water purification system (Millipore, MA). Phenol was water-saturated and equilibrated to pH 8 (Aquaphenol, MP Biomedicals, USA). Chloroform was a mixture of chloroform and isoamyl alcohol (24:1) (BioUltra, Supelco, Sigma-Aldrich, USA). The DNase I and RNase A enzymes and DAPI were purchased from Thermo Fisher Scientific (USA). Pure ATP standards for spiking were prepared from ATP standard of an ATP Colorimetric/Fluorometric Assay Kit (MAK190, Sigma-Aldrich, USA). Pure polyP standards for spiking were kindly given by RegeneTiss Inc. (P14, P60 and P130) or purchased from Sigma-Aldrich (P3) or Kerafast (P700). Silicone vacuum grease (High Vacuum Grease, Molykote, DuPont, USA) and all other chemicals were purchased from Sigma-Aldrich (USA).

C. reinhardtii strain and cultivation

The CC-4533 (CMJ030) strain was cultivated mixotrophically in a medium composed of 1 mM phosphate, 17.5 mM glacial acetic acid, Beijerinck's nutrient solution, 15 mM HEPES buffer and Kropat traces, adjusted to pH 7 with KOH, in 50 mL liquid cultures, under low constant illumination (~ 10 µmol photons·m^{-2}·s^{-1}) and constant agitation (130 rpm). Cultures were inoculated at 1–5 × 10^5 cells·mL^{-1} and let grow until log phase (0.5–3 × 10^6 cells·mL^{-1}), where they were maintained at least two days by dilutions before each experiment. Cells used for experiments were in log phase at ~ 2 × 10^6 cells·mL^{-1}.

For data normalisation, cell density in the culture was measured before each experiment with a haemocytometer after killing cells with 5% iodine tincture. To take into account potential losses of material in the harvesting steps, cell density was quantified again after harvesting with optical density measurements at 550 nm, using the conversion factor of 8.3 × 10^6 cells·$OD_{550}{}^{-1}$ we obtained by calibration of the measurement on CC-4533 [29]. Cell size distribution was obtained with a LUNA-FX7 (Logos Biosystems) cell counter.

Other microorganisms

The G49 strain, from the W303 background, of the yeast *Saccharomyces cerevisiae* was cultivated in YPD medium (1% yeast extract, 2% peptone, 2% dextrose) in the dark, at 30 °C and constant agitation (250 rpm). The strain was thawed one week before the experiment, and the culture was in logarithmic phase (OD_{600nm} = 0.6) when harvested. Cell density was calculated from optical density, using the conversion factor of 3.3 × 10^7 cells·mL^{-1}·$OD_{600}{}^{-1}$ obtained from calibration of the measurement, and coherent with the literature [29, 30].

The cyanobacteria *Synechococcus calcipolaris* (strain G9) and *Gloeomargarita lithophora* (strain C7) were cultivated in BG11 medium under constant illumination (5–10 µmol photons·m^{-2}·s^{-1}) at 30 °C and under constant agitation (100 rpm). The cultures were grown during 15 days to reach the logarithmic phase, between 1.1 and 3.2 OD_{730}. Cell density was calculated from optical density, using the conversion factors measured from calibration curves (8 × 10^7 cells·mL^{-1}·$OD_{730}{}^{-1}$ for C7 and 6 × 10^7 cells·mL^{-1}·$OD_{730}{}^{-1}$ for G9).

The CCMP1335 strain of the *Thalassiosira pseudonana* centric diatom was cultivated in ESAW medium (Enriched Seawater, Artificial Water) in light–dark cycles (12:12, 25 µmol photons·m^{-2}·s^{-1}) at 19 °C and without

agitation. The culture was grown for 4 days before reaching the log phase and was harvested at 2×10^6 cells·mL^{-1} at nine hours into the light phase of day 4.

The Pt1 strain of the *Phaeodactylum tricornutum* pennate diatom was cultivated in F/2 medium without agitation. The cultures were grown either synchronously in light–dark cycles (12:12, 25 µmol photons·m^{-2}·s^{-1}) at 19 °C for 4 days or under constant illumination (40 µmol photons·m^{-2}·s^{-1}) at 18 °C for 3 days. They were harvested at 3.1×10^6 cells·mL^{-1} at nine hours after the onset of light (for the light–dark condition) and at 5.1×10^6 cells·mL^{-1} (for the continuous light condition).

Harvesting methods

The following harvesting methods were used with the optimised extraction protocol for the experiments of Fig. 2. Harvesting methods are specified for each extraction protocol compared in Fig. 1 in the corresponding methods section. All other experiments were performed with direct pipetting and optimised extraction protocol.

Centrifugation

A volume of 1 mL of cell culture was centrifuged (5000 rcf, 5 min, 4 °C) in a 2 mL tube. The supernatant was discarded and the pellet was either directly resuspended in 750 µL ME buffer (25 mM 3-(N-morpholino)propanesulfonic acid (MOPS), 2.5 mM EDTA, pH 7) or in 1 mL of milliQ water to wash the cells. After washing, cells were pelleted with a second centrifugation with the same parameters, and either resuspended in 750 µL ME buffer or washed a second time before resuspension in 750 µL ME buffer. Finally, 600 µL of the ME buffer cell suspension were transferred to the extraction mix while the rest was used for chlorophyll fluorescence and cell density measurements.

Filtration

A volume of 1 mL of cell culture was filtered through a 3 µm mesh filter (Nuclepore Track-Etched Membranes, Whatman, USA) using a 15 mL glass filtration unit (Schott Duran, Germany) at 25 °C. A 50 mL syringe was used to slowly extract air from the lower compartment of the filtration unit, in order to prevent stressing the cells. For washing, cells were resuspended in 1 mL of milliQ water and filtered again. The filter was then inserted in a 2 mL tube and cells were collected with a flow of 750 µL ME buffer (25 mM MOPS, 2.5 mM EDTA, pH 7). Finally, 600 µL of cell suspension were transferred to the extraction mix while the rest was used for chlorophyll fluorescence and cell density measurements.

Direct pipetting

A volume of 600 µL of cell culture was directly transferred, at 25 °C and culture room illumination, from the culture to the extraction mix. Chlorophyll fluorescence and cell density were measured on cells directly pipetted from the culture.

Protocols published for ATP extraction

All steps were performed on ice or at 4 °C for centrifugation.

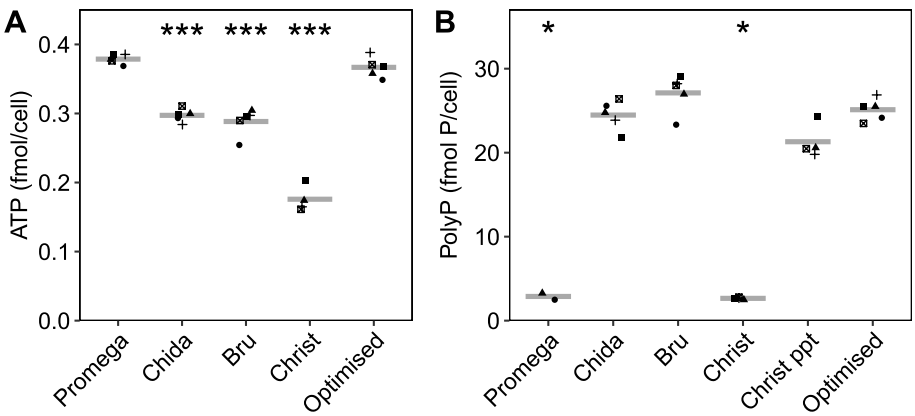


Fig. 1 Cellular concentrations of ATP and polyP after extractions with previously published protocols and the optimised protocol. ATP (**A**) and polyP (**B**) were assayed after metabolite extraction using phenol–chloroform ("Bru" (*24*), "Chida" (*21*), "Christ" (*25*) and optimised protocols) or TCA-based ("Promega") protocols, from the same CC-4533 culture. Four to five biological replicates of the same initial culture were measured. Three out of five replicates of the Promega protocol had non-measurable amounts of polyP. Grey crossbars indicate the mean values. "ppt" stands for precipitation of polyP after the Christ protocol. Stars represent significant differences compared to the optimised protocol (one-way ANOVA for ATP and Kruskal–Wallis test for polyP, corrected p-value coding: * $p < 0.05$, ** $p < 0.01$, *** $p < 0.001$)

"Chida" method (21)

A volume of 300 µL of cell culture was added to 1.5 mL of pre-cooled extraction mix (phenol–chloroform-water 6:2:2, 12 µl of 50 mM EDTA) in a 2 mL tube. After 20 s of vortexing, the tube was briefly centrifuged at 1000 rcf for 10 s and the lid was filled with silicone vacuum grease to easily separate the aqueous and organic phases. After centrifugation (12,000 rcf, 5 min), the aqueous phase was transferred to a pre-weighed 1.5 mL tube. The tube was weighed again to measure the exact extract volume and kept at − 20 °C until polyP precipitation and ATP quantification.

"Promega" method

The following TCA based extraction was performed according to the protocol supplied by the manufacturer (Enliten® ATP Assay System, Promega, USA). A volume of 400 µL of cell culture was added to 400 µL of cold 10% trichloroacetic acid (TCA). After 20 s of vortexing, the suspension was left on ice for ca. 1 h. After another 20 s vortexing, 400 µL of Tris–acetate (TA) buffer (10 mM Tris, 1 M acetate, pH 7.8) were added to the mix. The tube was centrifuged at 10,000 rcf for 5 min and 20 µL of the supernatant were transferred in a new 2 mL tube containing 1980 µL of TA buffer. 10 µL of the suspension was deposited on pH paper to verify neutrality (pH should be approximately 7.8). The sample was kept at − 20 °C until polyP precipitation and ATP quantification.

Protocols published for PolyP extraction

"Christ" method (25)

All steps were performed at room temperature (RT).

Cells were harvested by centrifugation (5000 rcf, 10 min) of 1 mL of culture in a 2 mL tube and washed twice in milliQ water. The pellet was resuspended in 500 µL ME buffer (25 mM MOPS, 2.5 mM EDTA, pH 7) and 100 µL were used for optical density measurement. 300 µL of phenol were added to the remaining 400 µL of suspension. After 20 s vortexing, the tube was incubated 10 min at 45 °C, cooled for 2 min on ice and briefly centrifuged. 1 mL of chloroform was added and vortexed 20 s to extract the phenol dissolved in the aqueous phase. After a brief centrifugation, the lid was filled with silicone vacuum grease. After centrifugation (12,000 rcf, 5 min), the aqueous phase was transferred to a new pre-weighed 1.5 mL tube. The tube was weighed again to measure the exact extract volume and kept at − 20 °C until ATP quantification and, when required, performing of a polyP precipitation (protocol "Christ ppt" in Fig. 1B).

"Bru" method (24)

Cells were harvested by centrifuging (5000 rcf, 5 min, 4 °C) 1 mL of culture in a 2 mL tube. The pellet was resuspended in 500 µL AE buffer (50 mM sodium acetate pH 5.3, 10 mM EDTA) and 100 µL were used for optical density measurement. Volumes of 300 µL of phenol and 40 µL of 10% SDS were added to the suspension. The tube content was homogenised (4 inversions and 5 s vortexing) and incubated 5 min at 65 °C, then cooled on ice for 1 min. A volume of 300 µL of chloroform was added before mixing again. The tube was briefly centrifuged at 1000 rcf for 10 s and the lid was filled with silicone vacuum grease. After centrifugation (13,000 rcf, 2 min, RT), the aqueous phase was transferred to a new 1.5 mL tube containing 500 µL of chloroform and mixed, then briefly centrifuged. The lid was filled with silicone vacuum grease. After centrifugation (13,000 rcf, 2 min, RT), the aqueous phase was transferred to a new pre-weighed 1.5 mL tube. The tube was weighed again to measure the exact extract volume. 3 µL of RNase A (10 $mg{\cdot}mL^{-1}$) and 3 µL of DNase I (10 $mg{\cdot}mL^{-1}$) were added and incubated 1 h at 37 °C. Samples were kept at − 20 °C until polyP precipitation and ATP quantification.

Optimised extraction protocol

All steps were performed on ice or at 4 °C for centrifugation.

A volume of 600 µL of cell culture was added to 1.2 mL of ice-cold extraction mix (phenol–chloroform 3:1, 12 µL of 50 mM EDTA) in a 2 mL tube. After 20 s vortexing, the tube was briefly centrifuged at 1000 rcf for 10 s and the lid was filled with silicone vacuum grease. After centrifugation (12,000 rcf, 5 min), the aqueous phase was transferred to a new 2 mL tube. One millilitre of chloroform was added and vortexed 20 s to extract the phenol dissolved in the aqueous phase. The tube was briefly centrifuged at 1000 rcf for 10 s and the lid was filled with silicone vacuum grease. After centrifugation (12,000 rcf, 5 min), the aqueous phase was transferred to a new pre-weighed 1.5 mL tube. The tube was weighed again to measure the exact extract volume and kept at − 20 °C until polyP precipitation and ATP quantification.

Physiology measurement with chlorophyll fluorescence

Chlorophyll fluorescence was used to measure the maximal yield of photosystem II (PSII) with a Speedzen fluorescence imaging setup (JBeamBio/API, France). A volume of 50 µL of cell suspension was put on a metallic plate and inserted in the Speedzen. The plate was left in the dark for 2 min prior to measurement, which consisted of minimal fluorescence (F_0) measurement in the dark and maximal fluorescence measurement (F_m) after a saturating pulse (2600 µmol photons m^{-2} s^{-1}, 250 ms of

green LEDs at 532 nm). The maximal PSII yield (Fv/Fm) was calculated using the formula of Eq. 1:

$$\frac{F_v}{F_m} = \frac{F_m - F_0}{F_m} \quad (1)$$

PolyP precipitation

A volume close to 300 µL of extract, corresponding to 0.5–1 10^6 cells, was used for polyP purification by ethanol precipitation. The precise volume of extract for precipitation was calculated for each sample to account for potential cell amount differences, in order to fall into the detection range of the polyP concentration assay. The calculated volume of extract was added to a pre-cooled 2 mL tube containing 2.5 volumes of cold 100% ethanol and 0.1 volume of 3 M sodium acetate (pH 5.3), and precipitation occurred overnight at − 20 °C, unless stated otherwise. After washing 1 min in 1 mL 70% ethanol, the pellet was dried at room temperature for 10 min, then resuspended in 220 µL of milliQ water.

Assays

ATP bioluminescent assay

ATP concentration in extracts was measured with the firefly Luciferin-Luciferase assay kit (Enliten ATP Assay System, Promega, USA). Extracts were diluted 100 times in ATP-free water. A volume of 100 µL of diluted extracts and pure ATP standards was pipetted onto a dark flat-bottom 96-well plate. Just before measurement, 100 µL of reagents were added to the measured well and mixed twice with the pipette. Measurements were performed in a CLARIOstar microplate reader (BMG Labtech, Germany). Luminescence at 555–70 nm was measured for 10 s to maximise signal detection.

PolyP spectrophotometric and fluorometric assays for concentration and average chain length

PolyP concentration in extracts was measured by enzymatic hydrolysis with scPpx1p and scIpp1p and spectrophotometric Pi detection, using the Phosfinity Total Polyphosphate Quantification Kit (Aminoverse, Netherlands) as described in [31]. Briefly, 100 µL of purified polyP and positive control were pipetted in two separate wells of a transparent flat-bottomed 96-well plate, as well as 100 µL of Pi standards and negative control. A volume of 50 µL of enzyme buffer was added to only one of the two wells of each sample and positive control. Then 50 µL of a premix of enzyme buffer and enzymes (49:1) were added to all the other wells. After mixing two times with a multichannel pipette, the plate was incubated 1 h at room temperature. A volume of 50 µL of detection solution (based on molybdate and ascorbate) was distributed to all wells and mixed twice with a multichannel pipette. The plate was inserted in the CLARIOstar microplate reader (BMG Labtech, Germany) and incubated 2 min at room temperature before reading absorbance at 882 nm.

PolyP average chain length was determined by hydrolysis of polyP down to $polyP_2$ with scPpx1p, conversion to ATP with ATP sulfurylase, then to glucose with hexokinase then to NADPH with glucose 6-phosphate dehydrogenase, and subsequent NADPH fluorometric detection, using the ChainQuant Polyphosphate Chain Length Determination Kit (Aminoverse, Netherlands) as described in [31]. Briefly, 100 µL of purified polyP were pipetted in two separate wells of a dark flat-bottomed 96-well plate, as well as 100 µL of $polyP_2$ standards and positive and negative controls in one well. 50 µL of a premix of enzyme buffer, additive and enzymes (44:5:1) without scPpx1p and ATP sulfurylase were added to only one of the two wells of each sample. A volume of 50 µL of a premix of enzyme buffer, additive and enzymes (44:5:1 or 42:5:3 for cell extracts) was added to all the other wells. Note that we only obtained consistent chain length results in our cell extracts when we tripled the enzyme amounts, probably because of the rather long (up to several thousand P) polyP chains in our samples. After mixing two times with a multichannel pipette, the plate was incubated 1 h at room temperature and 5 min in the microplate reader (CLARIOstar). Finally, the fluorescence was measured (excitation at 340–9 nm, emission at 460–9 nm).

Polyacrylamide gel electrophoresis of polyP extracts

Denaturing PAGE analysis of polyP extracts was carried out like in [32] with some modifications. PolyP standards (0.2 µg of P14, P60, P130 and P700) and three quantities (1 µg, 0.2 µg and 0.1 µg) of purified cell extract were loaded on a 4–18% polyacrylamide 8 M urea denaturing gel (13 cm height). As a reference, 1 µg of 1 kb + DNA ladder (N0550, New England Biolabs, USA) was also loaded. The gel was run overnight at 20 V and 3 h at 100 V. After a fixation step (30 min under mild agitation in the fixation buffer composed of 50 mM Tris–HCl pH 8, 25% methanol and 5% glycerol), the gel was stained in a bath containing 2 $\mu g \cdot mL^{-1}$ DAPI in the fixation buffer for 30 min, and destained in fixation buffer for 45 min. The gel was placed in a Gel Doc XR + Molecular Imager (Bio-Rad, USA) and UV illuminated until total bleaching of polyP-bound DAPI (10 min).

Data analysis and statistics

Data were treated by R scripts in RStudio. Statistical analysis included ANOVA and Tukey HSD tests for data with homogeneous variances (Figs. 1A, 2, 3 and 4) and Kruskal–Wallis and Dunn tests for data with non-homogeneous variances (Figs. 1B and 5). Variance homogeneity was tested with a Fisher's test.

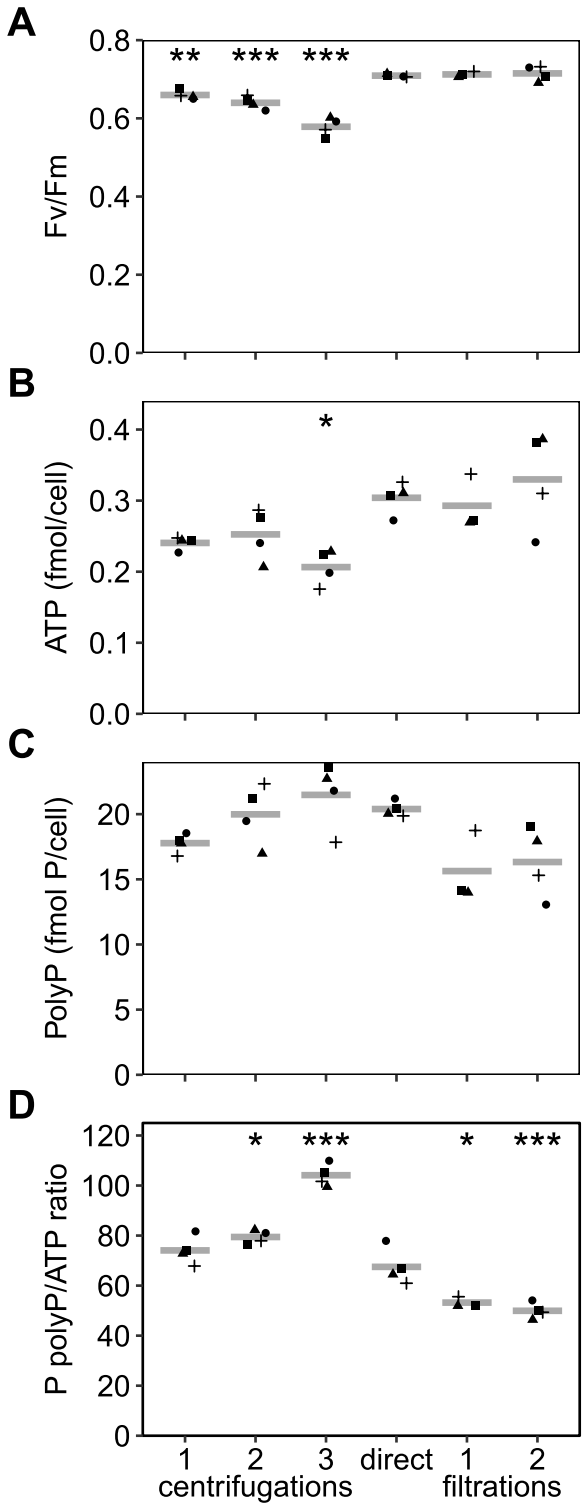


Fig. 2 Comparison of harvesting methods for ATP and polyP measurements. Cells were harvested by one or several rounds of centrifugation or slow filtration, or directly from the culture. Cells were washed with milliQ water between harvesting steps in the case of several centrifugations or filtrations, and ME buffer was used for the last resuspension of cells. After harvesting, fluorescence was measured to calculate the Fv/Fm ratio (**A**) and extraction with the optimised protocol was carried out to measure ATP (B), polyP (**C**) and calculate the polyP/ATP ratio (**D**). For photosynthesis measurement, samples of the "direct" protocol contained only culture solution, without EDTA. Four harvesting replicates (or three, for the 1 filtration protocol) of the same initial culture are shown. Grey crossbars indicate the mean values. Stars represent significant differences compared to direct harvesting (ANOVA: * $p < 0.05$, ** $p < 0.01$, *** $p < 0.001$)

Retrieved metabolite amounts in recovery experiments were calculated differently depending on the presence of cells in the medium. For ATP and polyP recovery rates from spiked fresh medium, we used Eq. 2:

$$Recovery\ \text{rate}\ (\%) = \frac{spiked\ extract\ (mol)}{spiked\ quantity\ (mol)} * 100 \quad (2)$$

ATP and polyP recovery rates from the spiked culture were calculated for each pair of spiked replicate i and unspiked replicate j, according to Eq. 3:

$$[Recovery\ \text{rate}\ (\%)]_{i,j} = \frac{[spiked\ extract\ (mol)]_i - [not\ spiked\ extract\ (mol)]_j}{spiked\ quantity\ (mol)} * 100 \quad (3)$$

Results

Comparison of different ATP and polyP extraction methods

To develop a joint ATP and polyP extraction method for *C. reinhardtii*, we compared different methods published for ATP or polyP extraction with our optimised protocol, designated as "optimised" protocol in the rest of the study (Fig. 1). ATP extraction protocols were either based on phenol–chloroform ("Chida" protocol, [21]) or TCA ("Promega" protocol, also published for *C. reinhardtii* in [20]), while polyP extraction protocols were all phenol–chloroform based ("Bru" protocol [24] and "Christ" protocol [25]). We considered that the best available protocols are those retrieving the highest amounts of each metabolite.

The optimised protocol performs as well as the best published protocols for each metabolite. For ATP extraction, the optimised protocol yields the same amount of ATP as the "Promega" protocol, whereas the "Chida", "Bru" and "Christ" protocols extract respectively 20, 20 and 50% less ATP than the optimised protocol (Fig. 1A). For polyP extraction, the "Christ" and "Promega" protocols perform significantly worse than the others,

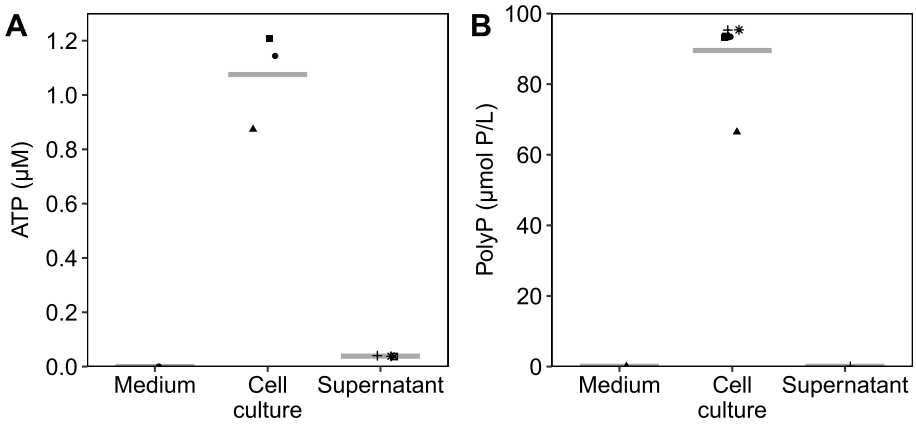


Fig. 3 PolyP and ATP are not found in the extracellular medium of a *C. reinhardtii* culture. ATP (**A**) and polyP (**B**) were extracted from equal volumes of fresh new medium, a log-phase cell culture and the supernatant of this culture after removing cells by centrifugation (5 min, 12,000 rcf). Three replicates for fresh medium and three to six replicates for cell and supernatant parts of the same culture are shown. Grey crossbars indicate mean values

retrieving hardly any polyP (Fig. 1B). The "Christ" protocol is originally a polyP extraction protocol that does not include a precipitation step. As we extracted 10 to 100 times less cells than in the publication, we did not need to dilute samples before quantification. We reasoned that phenol traces in our "Christ" extracts could be too high to allow proper quantification. We thus purified extracts from the "Christ" protocol before quantification (referred as "Christ ppt" in Fig. 1B). Adding this step allowed the "Christ" protocol to perform as well as the optimised, "Chida" and "Bru" protocols, showing that avoiding the polyP purification step is only possible when starting from high cell density samples and diluting the extract for polyP measurement.

Optimisation of cell harvesting

We compared three different harvesting approaches (Fig. 2). We harvested cells by (i) centrifugation with zero to two intermediate milliQ water washes, (ii) filtration with zero or one intermediate milliQ water wash and (iii) direct pipetting from the culture. To understand if differences in the retrieved ATP and polyP levels could be explained by changes in the physiological conditions caused by the different methods, we measured the PSII maximal yield (Fv/Fm) of the samples just before addition of the extraction mix. Indeed, the Fv/Fm ratio parameter lowers when cells experience hypoxia, which might occur in darkness or at high cell density during the harvesting [33].

Pipetting cell suspension directly from the culture to the extraction mix is the best harvesting protocol for cell physiology, ATP and polyP preservation (Fig. 2A-C).

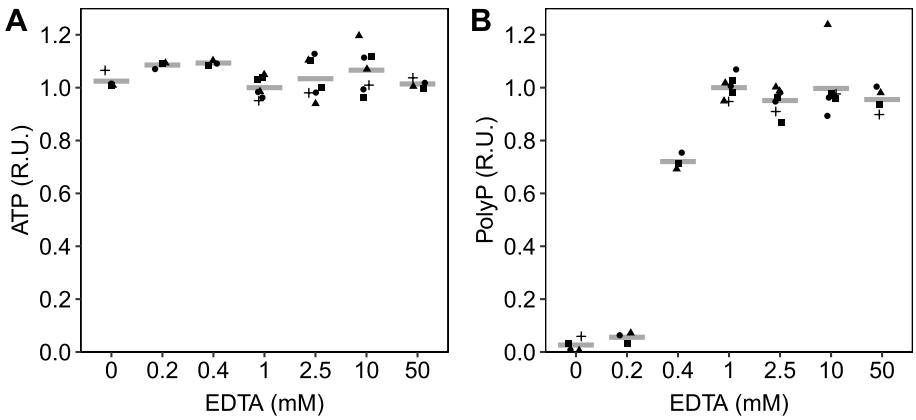


Fig. 4 Dependence on EDTA concentration of ATP and polyP extraction efficiency. ATP (**A**) and polyP (**B**) were extracted with the optimised protocol with different EDTA concentrations. Data from two independent experiments with respectively three and four biological replicates were normalised to the mean value at 1 mM EDTA. Grey crossbars indicate mean values

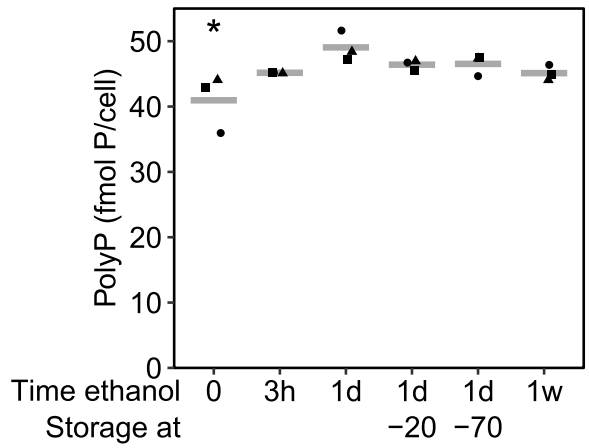


Fig. 5 Comparison of different methods for conservation post extraction. Cells were harvested and washed twice with milliQ water before extraction to avoid P contamination of the assay. For protocol "0", polyP were assayed directly after extraction. For all the other protocols, polyP were precipitated in ethanol. They were either stored in ethanol at − 20 °C for three hours ("3 h"), overnight ("1 d") or over one week ("1w"), and assayed directly after resuspension in water, or stored at − 20 °C ("− 20") or − 70 °C ("− 70") for one week before being measured. Three biological replicates are shown. Grey crossbars indicate the mean values. The star represents a significant difference compared to overnight precipitation (ANOVA, * $p < 0.05$)

Indeed, this protocol intrinsically allows to extract cells in the same physiological state as in the culture. We thus further compared the centrifugation and filtration protocols to this direct harvesting.

Filtration performs well, preserving the Fv/Fm ratio and retrieving the same amount of ATP as the direct protocol (Fig. 2A and B). Nevertheless, the polyP content after filtration is decreased by 25%, although non-significantly, compared to the direct harvesting (Fig. 2C). This could come from the mesh size of 3 µm, chosen to favour a quick filtration with limited turbulence for the cells, but which could let through the smallest cells or cell debris. We measured the cell size distribution of the CC- 4533 log-phase culture, and found that only 4% of the population have a size between 4 and 5 µm, while the rest are above 5.5 µm. If the 25% polyP loss would be imputable to these 4% of small cells, these cells would be enriched in polyP compared to the rest of the cell population.

Centrifugation is the least reliable technique to maintain ATP levels of *C. reinhardtii* cells, even when performed at 4 °C. One centrifugation is sufficient to decrease the Fv/Fm ratio (Fig. 2A), and the more centrifugations and washes, the larger the Fv/Fm decrease. The protocol with three centrifugations triggers a significant ATP decrease with 32% less ATP than with direct harvesting (Fig. 2B). The one and two centrifugation protocols also show a ~ 20% decrease in ATP compared to direct harvesting, although this is not statistically significant. On the contrary, centrifugation does not affect the polyP stocks (Fig. 2C), yielding comparable polyP concentrations to the direct harvesting protocol, whichever the number of centrifugations.

The physiological polyP/ATP ratio of CC- 4533 cells cultivated in mixotrophic conditions and at log-phase culture stage is around 70 (Fig. 2D). Harvesting by filtration leads to a lower ratio, due to decreased amounts of retrieved polyP. On the contrary, harvesting by centrifugation leads to a higher ratio, due to the decrease in ATP. The advantage of the joint extraction of ATP and polyP is obvious: while average coefficients of variation over all harvesting methods are 12% for ATP and 11% for polyP, the one of the ratio is twice lower at 6%.

We next evaluated if ATP or polyP are present as free metabolites in the culture medium, which would cause them to be harvested with the direct protocol. Indeed, extracellular polyP can be present in cell wall during cytokinesis in *C. reinhardtii* [34], and could end up in the medium. We thus checked the potential presence of ATP and polyP in the culture supernatant after centrifugation. No extracellular polyP and very low levels of extracellular ATP (< 4% of cellular levels) were retrieved, and they were both absent from fresh medium (Fig. 3).

Optimisation of the simultaneous ATP and polyP extraction method

To further improve the optimised protocol, we verified the effect of EDTA concentration on both ATP and polyP recovery from *C. reinhardtii*. We also investigated the conservation and precipitation conditions for polyP quantification.

EDTA is required for extraction of polyP, but does not affect ATP extraction (Fig. 4). Any concentration of EDTA above 1 mM is suitable for polyP extraction (Fig. 4, Panel B). The limit concentration of EDTA concentration is close to 0.4 mM, where ca. 30% less polyP are extracted than at 1 mM. Thus, 1 mM EDTA was chosen as the final concentration for the rest of this study. The EDTA concentration might be increased to ensure stability of samples with higher polyP contents.

Precipitation is required to retrieve the highest amount of polyP in our conditions (Fig. 5). To determine the effect of polyP precipitation, we harvested cells by centrifugation and washed them twice before carrying out the optimised extraction protocol. Samples that were not precipitated show a slightly lower amount of polyP compared to precipitation in ethanol. The time in ethanol or the freezer temperature of conservation after resuspension in water have no effect on the measured amounts of polyP. For practical reasons, extracts were precipitated during one day to one week and stored at − 20 °C for the rest of the study.

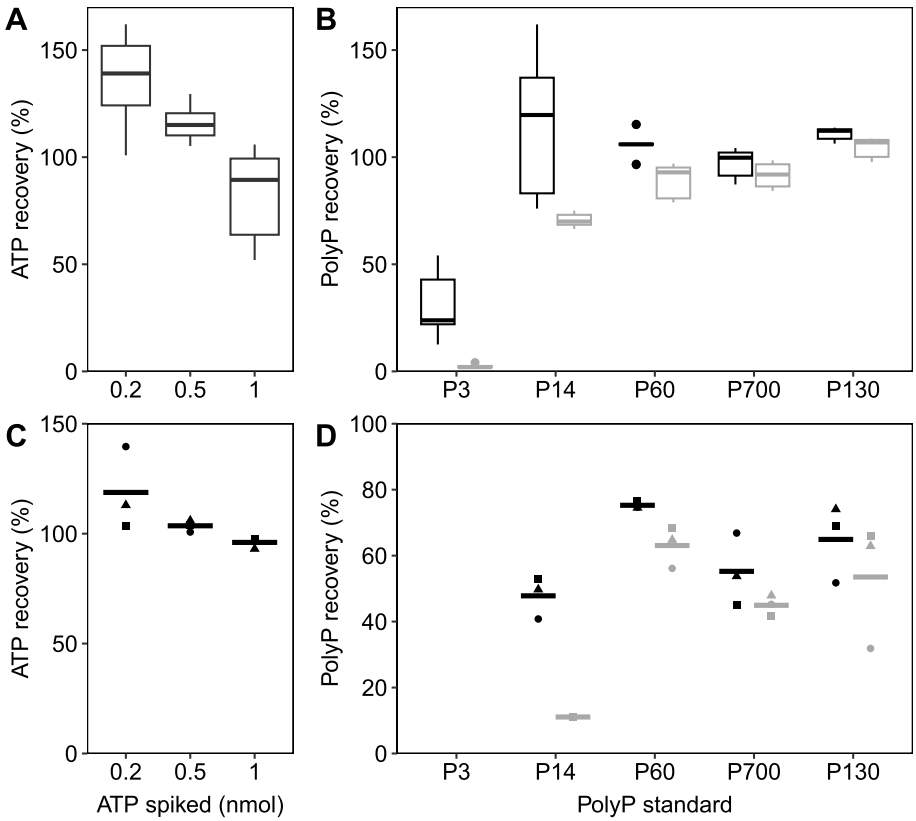


Fig. 6 ATP and polyP recovery after spiking before extraction. Extractions of pure ATP and polyP were done with (**A**, **B**) or without (**C**, **D**) CC-4533 cells. Three different quantities were introduced for ATP recovery (**A**, **C**) as shown on the x axis. Two different quantities were introduced for polyP recovery (**B**, **D**): 10 nmol P (black) and 50 nmol P (grey) alongside with five different polyP chain lengths as shown on the x axis. For extractions without cells, three biological replicates are shown and crossbars indicate mean values. For extractions with cells, boxplots represent the nine recovery rates calculated from cell extractions with and without spiking with three biological replicates each. Note that polyP standards are ordered according to their mean chain lengths and not their names. The star represents a significant difference of ATP recovery percentage compared to the theoretical 100% (one-sample t test, * $p < 0.05$)

Recovery of polyP and ATP after extraction

Using the optimised protocol, polyP and ATP recovery rates were tested in different conditions (Fig. 6). Three amounts (0.2 nmol, 0.5 nmol and 1 nmol ATP) of the ATP standard and two amounts (10 nmol and 50 nmol P as polyP) of five polyP standards (P3, P14, P60, P700, P130) were spiked in tubes already containing the extraction mix and either fresh medium or cell suspension. These spiking amounts were chosen to be close to or smaller than the amounts extractable from the cells they were mixed with. We tested conditions with and without cells, keeping in mind that these reconstitution systems with standards in solution introduced in culture medium can only partially mimic the biochemical environment and the structure of endogenous polyP and ATP during extraction. Please note that in Fig. 6B and 6D, we display the polyP standards in the order of their mean sizes measured with the chain length assay (Fig. 7).

ATP is fully recovered after the extraction with (Fig. 6A) or without cells (Fig. 6C). Smaller ATP quantities (0.2 and 0.5 nmol) are recovered with percentages higher than 100% in the cell containing experiments (136 and 116%, respectively), whereas all other conditions retrieve amounts not significantly different from 100%. This overestimation of the lower spiked ATP amounts is probably an artefact of the experiment. Indeed, since the spiking ATP was added to the homogenised phenol–chloroform-cell culture mix, it is impossible that more ATP was produced by cells in response to spiking.

PolyP full recovery is achieved in cell-containing environment for chains longer than 14 P units (Fig. 6B). Triphosphate (P3 in the figure) is not recovered at all (not measurable) when extracted in fresh medium (Fig. 6D) but partially (30% for 10 nmol and 0.2% for 50 nmol) recovered when extracted with cells (Fig. 6C). From P14 (10 nmol spiked) or P60 (50 nmol spiked), the retrieved

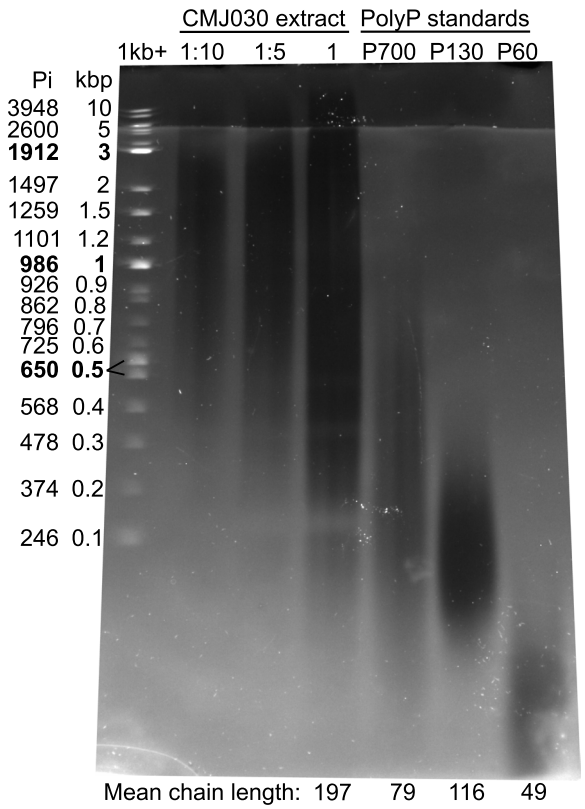


Fig. 7 Polyacrylamide gel of CC-4533 cell extract and polyP standards. Cell extract of twelve extraction replicates from the same culture were pooled, from which three quantities (1 µg, 0.2 µg and 0.1 µg) were loaded on a 4–18% polyacrylamide denaturing gel. A mass of 0.2 µg of three polyP standards and 1 µg of the 1 kb + DNA ladder (NEB) were also loaded for comparison. The depicted equivalent polyP chain lengths in P were calculated according to [35]. Mean chain lengths displayed at the bottom of the gel are the results of the chain length enzyme assay

polyP quantity is maximal, reaching 100% in the presence of cells and only ~70% without cells. Similar to ATP, polyP recovery rates are smaller with higher spiked polyP amounts, regardless of polyP sizes. Overall, polyP recovery rates are higher when extracted with cells than without.

Chain lengths of polyP extracted from CC- 4533

Given the apparent dependency to long chain of our extraction procedure, we measured the chain length of the extracted polyPs from *C. reinhardtii*. We ran polyP extracted from CC-4533 and commercial polyP standards on denaturing PAGE (Fig. 7).

The CC-4533 strain of *C. reinhardtii* produces a large range of sizes of polyP, spanning and sticking out of the zone covered by the 1 kbp + DNA ladder (equivalent to 246 to 3948 P units), with the maximal signal between 1000 and 2000 P residues. This is larger than the commercially available polyP standard P700, which contains the largest polyP chains. Signal intensity on the gel being related to mass, this technique is not well suited to evaluate the mean size of a polyP population. We thus quantified the mean chain lengths of the commercial standards and the CC-4533 extract with an enzyme assay [31]. P3, P14, P60 and P130 standards have mean chain lengths similar to their names, with respectively 3 P, 16 P, 49 P and 116 P. The P700 standard has a mean chain length of 79 P, much smaller than its label, which is consistent with the wide size distribution observed on the gel. PolyP extracted from CC-4533 have a mean chain length around 200 P.

PolyP and ATP extraction from different microorganisms

In order to show the versatility of the optimised method, we applied it to five other species: the model yeast *S. cerevisiae*, two model diatoms, the centric *T. pseudonana* and the pennate *P. tricornutum*, and the two cyanobacteria *G. lithophora* and *S. calcipolaris* (Table 1). All species were grown to logarithmic phase in standard conditions before extraction. *P. tricornutum* was grown either synchronously with 12 h:12 h light–dark cycles, like *T. pseudonana*, or asynchronously in constant light, like the other species.

Our protocol extracted both ATP and polyP from all species grown to log phase. ATP concentration has a limited range among the tested species (1 to 3 mM), while polyP concentrations differ greatly between species (15 to 519 mM). *G. lithophora* has the highest concentration of polyP, which is related to its numerous polyP granules [41], while *S. calcipolaris* and *T. pseudonana* have the lowest polyP concentrations. *P. tricornutum* has exactly the same ATP concentration in both synchronous low light (25 µmol photons·m^{-2}·s^{-1} in 12 h:12 h light–dark cycles) and asynchronous medium light (continuous 40 µmol photons·m^{-2}·s^{-1}) conditions, suggesting that in this species, ATP concentration does not depend on light intensity. Both culture conditions nevertheless show an almost fourfold difference in their polyP contents, polyP being much more accumulated in the synchronous culture under lower light.

The resulting polyP/ATP ratios reflect the same differences as the polyP measurements. *C. reinhardtii* and *S. cerevisiae* have very similar ratios around 70, while the other species have lower ratios with the exception of *G. lithophora*.

Discussion

We optimised a protocol to simultaneously and directly extract polyP and ATP from *C. reinhardtii* cells in culture. The method is simple to implement with four steps, and its efficiency compares with the published methods for polyP extraction optimised in other microeukaryotes

Table 1 ATP and polyP contents and polyP/ATP ratios in different microorganisms. The optimised protocol was applied on six log-phase cultures of five different microorganisms. ATP and polyP contents were quantified per cell and per volume, and used to calculate the polyP/ATP ratios. The average cell volumes to calculate concentrations were retrieved from the literature. Data for *C. reinhardtii* is the one of Fig. 2. Three or four biological replicates were used to calculate the displayed means and standard deviations in brackets. Sync: synchronised cultures growing in 12 h:12 h light–dark cycles

Species	Cell volume (μm^3)	Light ($\mu mol \cdot m^{-2} \cdot s^{-1}$)	ATP (fmol/cell)	ATP (mM)	polyP (fmol/cell)	polyP (mM)	polyP/ATP ratio
C. reinhardtii	300 [36]	10	0.304 (0.0227)	1.0 (0.08)	20.4 (0.59)	68 (2.0)	67 (7.3)
S. cerevisiae	60 [37]	-	0.080 (0.0072)	1.3 (0.12)	5.7 (0.28)	96 (4.6)	72 (6.1)
S. calcipolaris	4 [38]	5–10	0.010 (0.0005)	2.4 (0.12)	0.1 (0.01)	15 (2.2)	6 (1.1)
G. lithophora	4 [39]	5–10	0.006 (0.0002)	1.5 (0.06)	2.1 (0.05)	519 (13.5)	358 (20.2)
T. pseudonana	56 [40]	25, sync	0.166 (0.0051)	3.0 (0.09)	0.9 (0.25)	16 (4.4)	5 (1.6)
P. tricornutum	65 [40]	25, sync	0.109 (0.0017)	1.7 (0.03)	5.8 (0.64)	90 (9.8)	53 (5.4)
		40	0.109 (0.0043)	1.7 (0.07)	1.6 (0.16)	24 (2.4)	14 (1.8)

[24, 25, 42]. We identified some key parameters ensuring the efficiency of the method.

Direct harvesting and implications

Direct harvesting preserves the cell physiology as measured by the Fv/Fm ratio, and so does slow filtration (filtration and direct protocols, Fig. 2). On the contrary, PSII maximal yield is affected by our centrifugation protocol, where we centrifuge cells at 4 °C in order to slow down reactions involving ATP. During centrifugation, cells are in the dark for several minutes while they fall into hypoxia, becoming unable to produce ATP by mitochondrial respiration for a period of time three orders of magnitude above its life-time in the cell [27]. This and plain shear stress could explain the ~30% loss of ATP and the decrease of Fv/Fm after such treatment. Another possible stress could be the cold temperature we used in the centrifuge to slow down enzymatic reactions. Although short-term effects of cold stress have not yet been sufficiently studied, cells acclimated for one day at 4 °C have a two-fold reduced Fv/Fm and a more than two-fold starch increase [43, 44].

Direct harvesting from the culture allows to measure the cell ATP contents in physiological conditions, but imposes to work with the low polyP and ATP concentrations of the total culture. To counterbalance this dilution by the medium volume, polyP purification by ethanol precipitation allows to get rid of P contained in the medium and to concentrate the extracts for the quantification assay. Compared to the "Chida" protocol, our optimised protocol replaces water by cell suspension, allowing larger sample volumes to be extracted. This difference does not affect the extraction efficiency (see Fig. 1) and allows to double the number of extracted cells. Thus, with our method, it is possible to measure cell polyP content in low density samples, for example to follow polyP during a growth curve.

Need for phenol-devoid extracts

Extracts need to be clean of any phenol traces for both ATP and polyP quantification assays to work properly. The optimised protocol extracts significantly more ATP than the original "Chida" protocol (Fig. 1). The main difference between the two protocols is the additional chloroform extraction step, which allows to decontaminate the aqueous phase from phenol residuals [45]. The optimised protocol also extracts more ATP than the "Bru" protocol (Fig. 1) whereas it uses a second chloroform extraction step. This might be due to the use of DNase and RNase in the "Bru" protocol, leading to high amounts of nucleotides in the aqueous phase, which could interfere with the luciferase assay. For polyP, the additional chloroform extraction is also required, as can be seen by comparing the "Christ" extraction of Fig. 1B, using only one chloroform extraction and yielding 3 fmol polyP/cell, and the "0" condition of Fig. 5, using the optimised protocol with two chloroform extractions and no ethanol precipitation, and yielding 40 fmol polyP/cell. Additional polyP purification by ethanol precipitation is required to obtain the highest amounts of polyP, as shown in Figs. 5 and 1B. This is especially true if the polyP concentration in extracts is too low to necessitate further dilution for the assay, as performed in [25]. In the case of cultures at low concentration (lag or exponential phase), precipitation allows both to get rid of phenol traces that could inhibit the assay and to concentrate the extracts. Indeed, the "Christ" extraction protocol is less efficient for samples diluted five-fold or less (see Figs. 1 & 2 and [42]).

Filtration and spiking issues

Filtration retrieved 25% less polyP than direct harvesting of cells. It is improbable that this would come from a physiological degradation of polyP due to filtration, so this lost polyP-containing material could be soluble in the medium, contained in cell debris or in cells smaller than the filter pore size of 3 µm. The material that passes through the filter is pelleted in a 10 min, 5000 rcf centrifugation (see Fig. 2C) and in a 5 min, 12,000 rcf centrifugation (see Fig. 3B), so it cannot be soluble. We checked that the smallest cells in the culture were larger than 4 µm, coherent with the literature distribution between 4 and 13 µm for unsynchronised cultures [46]. Although we applied very low negative pressure for this filtration, it is probable that the 3 µm filter lets through the smallest cells and cell debris. The material lost by filtration represents 25% of polyP, but the first quartile of cell size in our cell population is 7 µm, a cell size that would not pass through the 3 µm filter. This means that the lost cells or cell debris are more concentrated in polyP than the average of cell population. The presence of polyP-rich debris or small cells will have to be further investigated with single cell techniques.

Our protocol retrieves less ATP and polyP when the spiked quantities are larger (Fig. 6). We used spiking amounts of ATP and polyP similar or lower to expected amounts in the co-extracted cells. It is hard to imagine that doubling the metabolite quantity to be extracted saturates the extractability capacity. This intriguing effect was already observed with a different method of extraction, without an explanation [47]. Whereas the presence of cells does not affect the recovery of spiked ATP by our extraction protocol, it favours the recovery of polyP. This could be due to stabilisation of polyP in the aqueous phase by the presence of other cell constituents, or to partial destabilisation of polyP in the ion-rich cell-free medium. Our spiking experiment intriguingly recovers more than 100% ATP with low spiking amounts in the presence of cells. We do not have a good explanation for this, and so did the authors of [47] with the same result on other metabolites. This issue in the spiking recovery experiment rationale will have to be further investigated to discriminate between technical and biochemical reasons.

PolyP size considerations

Since ethanol precipitation increases the measured amount of polyP (Fig. 5), probably due to the phenol removal effect, it is hard to know if any polyP material is lost during precipitation. Nevertheless, only very small chain polyP would be affected (see Fig. 6, only sizes < 14 P are recovered under 50%), which would not bias much the total P quantification in *C. reinhardtii* given the large size of its polyP (average size ~ 200 P units, see Fig. 7 and [48, 49]). However, we recommend to measure polyP size distribution of samples if the optimised method would be used with a different organism (e.g. [49] shows that *Phaeodactylum tricornutum* has especially short polyP with sizes inferior to 63 P units). The polyP concentrations we measured in the other microorganisms (Table 1) must therefore be taken with caution, as they might be underestimated due to loss of very short chain polyP (< 14 P) during extraction.

The majority of phosphate stored as polyP in CC-4533 is found in very long chains (up to several kP, Fig. 7 and [49]). Nevertheless, since the average chain length is around 200 P, the majority of polyP molecules in our samples must be quite short chains. To illustrate this consideration, we calculated that for one polyP chain of 4000 P, 20 chains of 5 P are required to get a 200 P average chain length in the sample. These 20 5P chains then represent only 2.5% of total P, but 95% of molecules. We thus interpret that the majority of small chains contained in our sample are not visible in the gel of Fig. 7. The presence of long (several kP) and short (< 100 P) polyP chains in our sample could reflect the different chemical forms under which polyP exist in *C. reinhardtii* cells, namely in solution or phase-separated as granules [50].

ATP and polyP levels in different species and culture conditions

ATP concentration differs only by a threefold factor between species, and remains in the mM range already identified in other cells (Table 1, [51]). Moreover, ATP levels are equal in our two samples of *P. tricornutum* cultivated at different light intensities and light regimes (Table 1). This represents very preliminary data suggesting that ATP concentration might be independent of environmental conditions in this microalgal species. This would make *P. tricornutum* similar to *S. cerevisiae,* which seems to have stable ATP levels during its cell cycle [52], while this is not the case for *E. coli* [53], where ATP levels vary depending on metabolism and cell cycle.

On the contrary to ATP, polyP concentrations vary by a 35-fold factor among species and cultivation conditions (Table 1). PolyP concentration measured in *S. cerevisiae* (96 mM, Table 1) is similar to the literature value obtained with the "Bru" protocol (95 mM, [24]) using standard growth conditions similar to ours, confirming the validity of our method with other microorganisms. The higher concentration of polyP in *G. lithophora* than in *S. calcipolaris* is also coherent with electron microscopy images showing less polyP granules in the latter [39, 41]. The two diatoms cultivated in the same conditions have very different polyP content, *P. tricornutum* cells accumulating 6.5 times more polyP than *T.*

pseudonana cells. Interestingly, *P. tricornutum* grown synchronously in 25 µmol photons·m^{-2}·s^{-1} accumulates 3.8 times more polyP than grown asynchronously at 40 µmol photons·m^{-2}·s^{-1}. Since both our samples were measured in log phase, we can hypothesise that light intensity and regime can lead to different polyP contents, maybe because of the growth limitation by carbon fixation. Our results are in the same range for *T. pseudonana* as in another study (0.9 compared to 0.8 fmol P/cell in [42]), but much higher for *P. tricornutum* (1.6 and 5.8 compared to 0.2 fmol P/cell in [42]). This difference could originate from method biases, polyP being very short in *P. tricornutum* (< 63 P) [49], or from cell cycle or culture conditions. Indeed, large polyP differences have been observed in the other diatom *Achnanthidium minutissimum* depending on P availability in the medium and on the growth curve stage [17].

Interest of the polyP/ATP ratio

Our method of harvesting and extraction for ATP and polyP allows to calculate the polyP/ATP ratio independently of any normalisation like cell density, chlorophyll concentration or dry mass measurement. Indeed, cell density measurement can become a problem if cells aggregate, for example in P and Ca deficiencies or if pH drifts too far from neutrality for *C. reinhardtii* [54]. Cell aggregation happened during the experiments of this study with the *C. reinhardtii* CC-4533 strain, although no harsh treatment was applied. Therefore, data dispersion is twice larger for ATP and polyP concentrations than for the polyP/ATP ratio in filtration and centrifugation-based extractions (Fig. 2). Since ATP concentrations do not vary much among species, the polyP/ATP ratio mainly reflects the storage of P as polyP. In conjunction with the ATP and polyP concentrations, the polyP/ATP ratio can thus be used to describe the polyP physiology of cells in various physiological and stress conditions. One could also use our method to diagnose the P storage level as polyP of complex natural populations.

Conclusion

We have devised an optimised protocol for the joint extraction of ATP and polyP from microorganisms, allowing to calculate the polyP/ATP ratio with precision. The method is efficient for both metabolites, except for very short chain polyP (chain lengths below 14 P). It can be used on low cell density samples, but requires purification steps allowing to get rid of the phenol in the extracts before measurements. Being based on the robust phenol–chloroform extraction, the method can readily be applied to follow the polyP physiology of diverse microorganisms grown in various physiological or stress culture conditions, or on natural microorganism samples. It can also be used to measure other metabolites extractable with phenol, and would represent a method of choice for other short-lived metabolites.

Abbreviations

ATP Adenosine triphosphate
PolyP Polyphosphates
TCA Trichloroacetic acid

Acknowledgements

EI and AB thank Yves Choquet and Emanuel Sanz-Luque for fruitful discussions and suggestions to improve the optimised protocol, Aurélia Barascu for her kind provision of *S. cerevisiae*, Fériel Skouri-Panet for her kind provision of *S. calcipolaris* and *G. lithophora*, Raphaël Monteil for his kind provision of *P. tricornutum*, Emeline Verney for her kind provision of *T. pseudonana*, Mathias Penot-Raquin and Richard Dorrell for giving us access to their LUNA-FX7 cell counter, Irelka Colina for her advice on statistical analysis, and Stephan Eberhard and Benjamin Bailleul for helpful and insightful comments on the manuscript.

Authors' contributions

AB conceived and supervised the project. AB and EI designed the experiments. EI performed experiments, analysed the data and wrote the manuscript. AB and EI corrected and approved the final manuscript.

Funding

The ANR grant Phosphalgue (ANR-21-CE43-0021) funded the research performed in this article and the PhD salary of EI. The research presented here also benefited from recurrent funding from the CNRS and Sorbonne Université to the lab, as well as the "Initiative d'Excellence" program (Grant "DYNAMO," ANR-11-LABX-0011-01).

Data availability

All data generated or analysed during this study are included in this published article.

Declarations

Ethics approval and consent to participate

Not applicable.

Consent for publication

Not applicable.

Competing interests

The authors declare no competing interests.

Author details

[1]Photobiology and Physiology of Plastids and Microalgae, CNRS – Sorbonne Université, Paris 75005, France.

Received: 16 December 2024 Accepted: 7 April 2025
Published online: 26 May 2025

References

1. Glonek T. Did cyclic metaphosphates have a role in the origin of life? Orig Life Evol Biosph. 2021;51:1–60.
2. Sanz-Luque E, Bhaya D, Grossman AR. Polyphosphate: A multifunctional metabolite in cyanobacteria and algae. Front Plant Sci. 2020;11:938.
3. Denoncourt A, Downey M. Model systems for studying polyphosphate biology: a focus on microorganisms. Curr Genet. 2021;67:331–46.
4. Sanz-Luque E, Saroussi S, Huang W, Akkawi N, Grossman A. R. Metabolic control of acclimation to nutrient deprivation dependent on polyphosphate synthesis. Sci Adv. 2020;6:eabb5351.
5. Kornberg A, Rao NN, Ault-Riché D. Inorganic polyphosphate: a molecule of many functions. Annu Rev Biochem. 1999;68:89–125.
6. Liu W, Wang J, Comte-Miserez V, Zhang M, Yu X, Chen Q, Jessen HJ, Mayer A, Wu S, Ye S. Cryo-EM structure of the polyphosphate polymerase VTC

reveals coupling of polymer synthesis to membrane transit. The EMBO J. 2023;42: e113320.
7. Le Moigne T, Boisset N. D., de Carpentier F, Crozet P, Danon A, Henri J, Marchand C. H., Lemaire S. D., Johnson X, "Chapter 8 - Photoproduction of reducing power and the Calvin-Benson cycle" in The Chlamydomonas Sourcebook (Third Edition), A. R. Grossman, F.-A. Wollman, Eds. (Academic Press, London, 2023; https://www.sciencedirect.com/science/article/pii/B978012821430500016X), pp. 273–315.
8. Deschamps P, Ball S. G., Dauvillée D, "The comparative, biochemistry, genetics, and evolution of starch metabolism in *Chlamydomonas reinhardtii*" in The Chlamydomonas Sourcebook (Third Edition), A. R. Grossman, F.-A. Wollman, Eds. (Academic Press, London, 2023; https://www.sciencedirect.com/science/article/pii/B9780128214305000031), pp. 23–50.
9. Posewitz M. C., Atteia A, Hemschemeier A, Happe T, Grossman A. R. "Chapter 9 - Metabolic networks during dark anoxia" in The Chlamydomonas Sourcebook (Third Edition), A. R. Grossman, F.-A. Wollman, Eds. (Academic Press, London, 2023; https://www.sciencedirect.com/science/article/pii/B9780128214305000195), pp. 317–341.
10. Weeks D. P. "Genetic transformation of Chlamydomonas nuclear, chloroplast, and mitochondrial genomes" in The Chlamydomonas Sourcebook (Third Edition), U. Goodenough, Ed. (Academic Press, 2023; https://www.sciencedirect.com/science/article/pii/B9780128224571000182), pp. 325–343.
11. Baidukova O, Kelterborn S, Sizova I, Hegemann P. "Chapter 17 - Reverse genetics" in The Chlamydomonas Sourcebook (Third Edition), U. Goodenough, Ed. (Academic Press, 2023; https://www.sciencedirect.com/science/article/pii/B978012822457100011X), pp. 421–430.
12. P. Crozet, F. J. Navarro, F. Willmund, P. Mehrshahi, K. Bakowski, K. J. Lauersen, M.-E. Pérez-Pérez, P. Auroy, A. Gorchs Rovira, S. Sauret-Gueto, J. Niemeyer, B. Spaniol, J. Theis, R. Trösch, L.-D. Westrich, K. Vavitsas, T. Baier, W. Hübner, F. de Carpentier, M. Cassarini, A. Danon, J. Henri, C. H. Marchand, M. de Mia, K. Sarkissian, D. C. Baulcombe, G. Peltier, J.-L. Crespo, O. Kruse, P.-E. Jensen, M. Schroda, A. G. Smith, S. D. Lemaire, Birth of a photosynthetic chassis: A MoClo toolkit enabling synthetic biology in the microalga *Chlamydomonas reinhardtii*. ACS Synth Biol. 2018;7:2074–2086.
13. Crimp A, Brown N, Shilton A. Microalgal luxury uptake of phosphorus in waste stabilization ponds - frequency of occurrence and high performing genera. Water Sci Technol. 2018;78:165–73.
14. Zúñiga-Burgos T, Saiardi A, Camargo-Valero M. A, Baker A. Phosphate overplus response in *Chlamydomonas reinhardtii*: polyphosphate dynamics to monitor phosphate uptake and turnover. bioRxiv [Preprint]. 2024. https://doi.org/10.1101/2024.01.25.577272.
15. Plouviez M, Fernández E, Grossman AR, Sanz-Luque E, Sells M, Wheeler D, Guieysse B. Responses of *Chlamydomonas reinhardtii* during the transition from P-deficient to P-sufficient growth (the P-overplus response): The roles of the vacuolar transport chaperones and polyphosphate synthesis. J Phycol. 2021;57:988–1003.
16. Diaz JM, Steffen R, Sanders JG, Tang Y, Duhamel S. Preferential utilization of inorganic polyphosphate over other bioavailable phosphorus sources by the model diatoms *Thalassiosira spp*. Environ Microbiol. 2019;21:2415–25.
17. Lapointe A, Kocademir M, Bergman P, Ragupathy IC, Laumann M, Underwood GJC, Zumbusch A, Spiteller D, Kroth PG. Characterization of polyphosphate dynamics in the widespread freshwater diatom *Achnanthidium minutissimum* under varying phosphorus supplies. J Phycol. 2024. https://doi.org/10.1111/jpy.13423.
18. Zhang F, Wen Z, Wang S, Tang W, Luo Y-W, Kranz SA, Hong H, Shi D. Phosphate limitation intensifies negative effects of ocean acidification on globally important nitrogen fixing cyanobacterium. Nat Commun. 2022;13:6730.
19. Lundin A, Thore A. Comparison of methods for extraction of bacterial adenine nucleotides determined by firefly assay. Appl Microbiol. 1975;30:713–21.
20. Finazzi G, Furia A, Barbagallo R. P., Forti G. State transitions, cyclic and linear electron transport and photophosphorylation in *Chlamydomonas reinhardtii*. Biochimica et Biophysica Acta (BBA) – Bioenergetics. 1999;1413:117–129.
21. Chida J, Yamane K, Takei T, Kido H. An efficient extraction method for quantitation of adenosine triphosphate in mammalian tissues and cells. Anal Chim Acta. 2012;727:8–12.
22. Kumble KD, Kornberg A. Inorganic polyphosphate in mammalian cells and tissues. J Biol Chem. 1995;270:5818–22.
23. Wood HG, Clark JE. Biological aspects of inorganic polyphosphates. Annu Rev Biochem. 1988;57:235–60.
24. Bru S, Jimenez J, Canadell D, Arino J, Clotet J. Improvement of biochemical methods of polyP quantification. Microb Cell. 2017;4:6–15.
25. Christ JJ, Blank LM. Analytical polyphosphate extraction from *Saccharomyces cerevisiae*. Anal Biochem. 2018;563:71–8.
26. Cakmak T, Angun P, Demiray YE, Ozkan AD, Elibol Z, Tekinay T. Differential effects of nitrogen and sulfur deprivation on growth and biodiesel feedstock production of *Chlamydomonas reinhardtii*. Biotechnol Bioeng. 2012;109:1947–57.
27. Stitt M, Wirtz W, Heldt HW. Metabolite levels during induction in the chloroplast and extrachloroplast compartments of spinach protoplasts. Biochem Biophys Acta. 1980;593:85–102.
28. Mettler T, Mühlhaus T, Hemme D, Schöttler M-A, Rupprecht J, Idoine A, Veyel D, Pal SK, Yaneva-Roder L, Winck FV, Sommer F, Vosloh D, Seiwert B, Erban A, Burgos A, Arvidsson S, Schönfelder S, Arnold A, Günther M, Krause U, Lohse M, Kopka J, Nikoloski Z, Mueller-Roeber B, Willmitzer L, Bock R, Schroda M, Stitt M. Systems analysis of the response of photosynthesis, metabolism, and growth to an increase in irradiance in the photosynthetic model organism *Chlamydomonas reinhardtii*. Plant Cell. 2014;26:2310–50.
29. Myers JA, Curtis BS, Curtis WR. Improving accuracy of cell and chromophore concentration measurements using optical density. BMC Biophys. 2013;6:4.
30. Fukuda N. Apparent diameter and cell density of yeast strains with different ploidy. Sci Rep. 2023;13:1513.
31. Christ JJ, Willbold S, Blank LM. Polyphosphate chain length determination in the range of two to several hundred P-subunits with a new enzyme assay and 31 P NMR. Anal Chem. 2019;91:7654–61.
32. Smith SA, Morrissey JH. Sensitive fluorescence detection of polyphosphate in polyacrylamide gels using 4',6-diamidino-2-phenylindol. Electrophoresis. 2007;28:3461–5.
33. Bulté L, Gans P, Rebéillé F, Wollman F-A. ATP control on state transitions *in vivo* in *Chlamydomonas reinhardtii*. Biochimica et Biophysica Acta (BBA) – Bioenergetics. 1990;1020:72–80.
34. Werner TP, Amrhein N, Freimoser FM. Inorganic polyphosphate occurs in the cell wall of *Chlamydomonas reinhardtii* and accumulates during cytokinesis. BMC Plant Biol. 2007;7:51.
35. Smith SA, Wang Y, Morrissey JH. DNA ladders can be used to size polyphosphate resolved by polyacrylamide gel electrophoresis. Electrophoresis. 2018;39:2454–9.
36. Zhang N, Pazouki L, Nguyen H, Jacobshagen S, Bigge BM, Xia M, Mattoon EM, Klebanovych A, Sorkin M, Nusinow DA, Avasthi P, Czymmek KJ, Zhang R. Comparative phenotyping of two commonly used *Chlamydomonas reinhardtii* background strains: CC-1690 (21gr) and CC-5325 (the CLiP mutant library background). Plants (Basel). 2022;11:585.
37. Petrezselyova S, Zahradka J, Sychrova H. Saccharomyces cerevisiae BY4741 and W303–1A laboratory strains differ in salt tolerance. Fungal Biol. 2010;114:144–50.
38. Li J, Margaret Oliver I, Cam N, Boudier T, Blondeau M, Leroy E, Cosmidis J, Skouri-Panet F, Guigner J-M, Férard C, Poinsot M, Moreira D, Lopez-Garcia P, Cassier-Chauvat C, Chauvat F, Benzerara K. Biomineralization patterns of intracellular carbonatogenesis in cyanobacteria: Molecular hypotheses. Minerals. 2016;6:10.
39. Moreira D, Tavera R, Benzerara K, Skouri-Panet F, Couradeau E, Gérard E, Fonta C. L., Novelo E, Zivanovic Y, López-García P. Description of *Gloeomargarita lithophora gen. nov., sp. nov.*, a thylakoid-bearing, basal-branching cyanobacterium with intracellular carbonates, and proposal for *Gloeomargaritales ord. nov*. Int J System Evol Microbiol. 2017;67:653–658.
40. Thompson PA, Harrison PJ, Parslow JS. Influence of irradiance on cell volume and carbon quota for ten species of marine phytoplankton. J Phycol. 1991;27:351–60.
41. Benzerara K, Skouri-Panet F, Li J, Férard C, Gugger M, Laurent T, Couradeau E, Ragon M, Cosmidis J, Menguy N, Margaret-Oliver I, Tavera R, López-García P, Moreira D. Intracellular Ca-carbonate biomineralization is widespread in cyanobacteria. Proc Natl Acad Sci U S A. 2014;111:10933–8.
42. Lapointe A, Spiteller D, Kroth PG. High throughput method for extracting polyphosphates from diatoms. Endocytosis and Cell Research. 2022;31:29–38.

43. Valledor L, Furuhashi T, Hanak A-M, Weckwerth W. Systemic cold stress adaptation of *Chlamydomonas reinhardtii*. Mol Cell Proteomics. 2013;12:2032–47.
44. Ermilova E. Cold stress response: An overview in Chlamydomonas. Front Plant Sci. 2020;11: 569437.
45. Toni LS, Garcia AM, Jeffrey DA, Jiang X, Stauffer BL, Miyamoto SD, Sucharov CC. Optimization of phenol-chloroform RNA extraction MethodsX. 2018;5:599–608.
46. Liu D, Vargas-García CA, Singh A, Umen J. A cell-based model for size control in the multiple fission alga *Chlamydomonas reinhardtii*. Curr Biol. 2023;S0960–9822(23):01409–14.
47. Arrivault S, Guenther M, Ivakov A, Feil R, Vosloh D, van Dongen JT, Sulpice R, Stitt M. Use of reverse-phase liquid chromatography, linked to tandem mass spectrometry, to profile the Calvin cycle and other metabolic intermediates in Arabidopsis rosettes at different carbon dioxide concentrations. The Plant journal : for cell and molecular biology. 2009;59:826–39.
48. Li Y, Chen S, Liu N, Ma L, Wang T, Veedu RN, Li T, Zhang F, Zhou H, Cheng X, Jing X. A systematic investigation of key factors of nucleic acid precipitation toward optimized DNA/RNA isolation. Biotechniques. 2020;68:191–9.
49. Leitão JM, Lorenz B, Bachinski N, Wilhelm C, Müller WEG, Schröder HC. Osmotic-stress-induced synthesis and degradation of inorganic polyphosphates in the alga *Phaeodactylum tricornutum*. Mar Ecol Prog Ser. 1995;121:279–88.
50. Goodenough U, Heiss AA, Roth R, Rusch J, Lee J-H. Acidocalcisomes: Ultrastructure, biogenesis, and distribution in microbial eukaryotes. Protist. 2019;170:287–313.
51. Greiner JV, Glonek T. Intracellular ATP concentration and implication for cellular evolution. Biology (Basel). 2021;10:1166.
52. Takaine M, Ueno M, Kitamura K, Imamura H, Yoshida S. Reliable imaging of ATP in living budding and fission yeast. Journal of Cell Science. 2019;132:jcs230649.
53. Lin W-H, Jacobs-Wagner C. Connecting single-cell ATP dynamics to overflow metabolism, cell growth, and the cell cycle in *Escherichia coli*. Curr Biol. 2022;32:3911-3924.e4.
54. de Carpentier F, Lemaire SD, Danon A. When unity is strength: The strategies used by Chlamydomonas to survive environmental stresses. Cells. 2019;8:1307.

Publisher's Note

Springer Nature remains neutral with regard to jurisdictional claims in published maps and institutional affiliations.